Elastic registration vs. block matching for quantification of cardiac function with 3D ultrasound: initial results of a direct comparison in silico based on a new evaluation pipeline

Martino Alessandrini*, Brecht Heyde*, Szymon Cygan†, Maxime Sermesant‡, Hervé Delingette‡, Olivier Bernard§ Mathieu De Craene¶ and Jan D'hooge*‖
*Department of Cardiovascular Imaging and Dynamics, KULeuven, Leuven, Belgium.
†Politechnika Warszawska, Instytut Metrologii i Inzynierii Biomedycznej WydzialMechatroniki, Warsaw, Poland.
‡Asclepios Res. Project, INRIA, Sophia Antipolis, Cedex, France.
§Université de Lyon, CREATIS, CNRS UMR5220, INSERM U1044, Université Lyon 1, INSA-LYON, Villeurbanne, France.
¶Medisys, Philips Research Paris, Paris, France.
‖Department of Circulation and Medical Imaging, Norges teknisk-naturvitenskapelige universitet, Trondheim, Norway.

***Abstract*—This paper presents a comparison between block matching and elastic registration for the estimation of cardiac deformation and strain from 3D ultrasound. The comparison study exploits a new evaluation pipeline recently developed by the authors. The pipeline generates synthetic sequences that are extremely similar to real ultrasound recording while the synthetic cardiac motion is fully controlled by an electro-mechanical model of the heart. Hereto, five synthetic sequences were generated corresponding to one healthy heart and four ischemic ones. Elastic registration returned both the smaller tracking errors and the most robust strain estimates. Although with limitations, this study brings further evidence that the new technique might be ready for extensive clinical testing.**

I. Introduction

Cardiac strain quantification from 3D ultrasound is an active area of research. Commercially available solutions for strain estimation are mainly based on block-matching (BM). Recently, techniques based on elastic registration [2] have also been proven feasible although still confined to the research arena and less extensively tested. Hereto, initial comparison studies recently showed that elastic registration is potentially more accurate BM as far as 2D strain is concerned [1], [3]. Surprisingly, a thorough and reproducible comparison between the two solutions on 3D ultrasound is to date still missing likely, in part, due to the lack of a solid benchmarking framework.

In this context, we have recently proposed a pipeline for the quality assurance of strain estimation techniques *in silico*. The pipeline generates synthetic 3D echocardiographic sequences which looks extremely similar to real ultrasound recordings, while the synthetic cardiac motion is fully controlled by an advanced electro-mechanical model of the heart [4].

In this study, the new pipeline is employed to perform an initial comparison between BM and elastic registration techniques. Hereto, five synthetic datasets were generated including one healthy motion pattern and four ischemic. The two techniques were then compared in terms of tracking accuracy and strain estimation. The capability of discriminating between healthy and akinetic segments were also assessed. The paper proceeds as follows. Sect. II briefly introduces the evaluation pipeline, presents the two algorithms considered and describes the adopted performance metrics. Sect. III reports the results while Sect. IV discusses the limitations of the study, draws the conclusions and presents future perspectives.

II. Materials and Methods

A. Evaluation Pipeline

The evaluation pipeline was recently presented in [4]. It combines state-of-the art solutions in the fields of electromechanical modeling [5] and ultrasound simulation [6] within an original framework that exploits a real ultrasound recording to learn and simulate realistic speckle textures. The simulated images show typical artifacts that make motion tracking in ultrasound challenging. Moreover, the ground-truth displacement field is available voxelwise and is fully controlled by the electromechanical model.

By varying the value of the parameters of the E/M simulator [5] a library of five cases was created including one healthy heart and four ischemic. The healthy case was generated by assigning normal contractility and stiffness values to all heart segments, as defined by the American Heart Association (AHA) 17 segments model [7]. The ischemic cases were then simulated by modifying peak contractility and stiffness values in diseased segments by differentiating between fully ischemic and mildly ischemic segments. The four ischemic cases corresponded to occlusions of the distal segment of the Left Anterior Descending (LADdist) artery, of the proximal occlusion of the same artery (LADprox), of the Right Coronary Artery (RCA) and of the Left Circumflex artery (LCX), cf. [8] for more details.

A synthetic system with the following characteristics was implemented in the ultrasound simulator [6]: sampling frequency 50 MHz, center frequency of the probe 3.3 MHz with a -6 dB relative bandwidth of 65%, static focusing at 80 mm

when transmitting and dynamically focusing on receive. The simulated images consisted of 107×80 lines in azimuth and elevation direction over an angle of 76×76 degrees, resulting in a frame rate of 30 Hz assuming parallel beam forming and ECG gating. After scan-conversion each volume measured 208×176×208 pixels^3 (voxel size 0.6×0.8×0.5 mm^3).

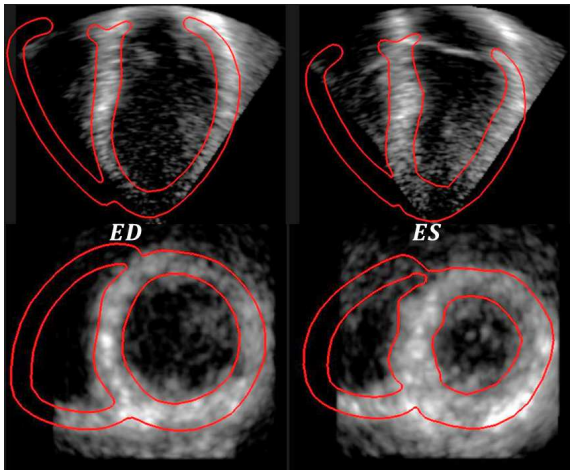

Fig. 1. End diastolic and end-systolic frames from the healthy simulation. In red the boundary of the ground-truth meshes providing reference values of displacement and strain.

An example of simulated sequence is provided in Fig. 1. An animation showing one full sequence can be found at http://bit.ly/sim_us.

B. Considered Algorithms

All five simulated sequences were processed by the two motion estimation techniques considered.

1) Elastic Registration: The technique in [2] was considered as representative of the elastic registration family. In its formalism, the inter-frame displacement field $\mathbf{u} = \mathbf{u}(x, y, z)$ is expressed as:

$$\mathbf{u} = \sum_{i,j,k} \mu_{i,j,k} \beta \left(\frac{x - \kappa_x^i}{\sigma_x} \right) \beta \left(\frac{y - \kappa_y^j}{\sigma_y} \right) \beta \left(\frac{z - \kappa_z^k}{\sigma_z} \right) \quad (1)$$

being β the third order B-spline, κ_ξ the node spacing and σ_ξ the node span. Parameters $\mu_{i,j,k}$ are optimized with the LBFGSB optimizer by minimizing the cost function:

$$E = \sum_{\mathbf{r}} \| I_n(\mathbf{r}) - I_{n+1}(\mathbf{T}(\mathbf{r})) \|^2 + \alpha \sum_{\mathbf{r}} \left\| \frac{\partial^2 \mathbf{T}(\mathbf{r})}{\partial \mathbf{r}^2} \right\|^2 \quad (2)$$

where $\mathbf{T}(\mathbf{r}) = \mathbf{r} + \mathbf{u}(\mathbf{r})$ and α is the hyperparameter to modulate the influence of the bending energy.

As opposed to previous works where control points were put on a Cartesian grid, an original anatomical grid topology is employed in [2], specifically adapted to the geometry of the considered ventricular shape. With respect to the Cartesian topology, the novel technique was shown to be competitive in terms of estimation accuracy while computationally more effective, cf. [2].

2) Block matching: Block matching employed 3D Normalized Cross-Correlation (NCX) as similarity metric. Prior to localizing the maximum of the resulting NCX it was interpolated in 3D by recursively (3 times) interleaving interpolates between every element using the cubic B-spline method, which resulted in 8-times improved spatial resolution of displacements estimates. The search range for each block matching was set globally to cover maximum physiological velocities in cardiac motion of 12cm/s. Dimensions of matched blocks (kernels) were chosen experimentally by assessing the average and median errors of displacements estimation for various kernel sizes. Here the kernel was 14.3 × 18 × 12.3 mm^3. No smoothing, regularization or quality check measures were implemented.

C. Performance Evaluation

For each sequence, the result of each estimator was applied to progressively track the 5387 nodes of the first simulation mesh over the whole cardiac cycle. Tracking accuracy was then evaluated by measuring the Euclidean distance to the nodes of the ground truth meshes. In particular, for each technique we evaluated global tracking error (*i.e.* inclusive of all nodes and time instants), instantaneous tracking error (*i.e.* inclusive of all nodes at a specific time instant) and local tracking error maps evaluated at end-systole (ES).

From the sets of volumetric meshes, strain values were obtained by approximating the displacement within each tetrahedron as an affine transform $\mathbf{F}$. The Green-Lagrange strain tensor $\mathbf{E} = 1/2 \left(\mathbf{F}^T \mathbf{F} - \mathbf{I} \right)$ was then computed and projected on the local cardiac coordinate system of longitudinal (L-strain), radial (R-strain) and circumferential (C-strain) directions according to $\epsilon_d = \mathbf{d}^T \mathbf{E} \mathbf{d}$. Being $\mathbf{d} = [d_1, d_2, d_3]^T$ the unit vector for the anatomical coordinate of interest. Segmental strain values were then obtained by averaging the point estimates for each AHA segment.

For each algorithm we evaluated the accuracy in recovering ES strain (the most relevant from a clinical perspective). Hereto, Pearson correlation coefficient together with the bias and standard deviation returned by the Bland-Altman (BA) analysis were used. For each correlation value the p-value was computed testing the hypothesis of no correlation. The statistical significance of each reported bias was measured with a t-test. Fishers z-transform was used to compare the strengths of different correlations. A t-test was used to compare the biases returned by the BA analysis. Differences were considered statistically significant if $p<0.05$.

III. Results

A. Tracking accuracy

Boxplots of the global tracking error are reported in Fig. 2. Elastic registration was on average more accurate than block matching on all sequences considered. On the entire dataset, global tracking error was ($\mu \pm \sigma$) 1.153±0.625 mm for elastic registration and 1.612±1.161 for block matching. The same behavior was observed when considering the time evolution of the tracking error, cf. Fig. 3.

Besides smaller average errors, elastic registration returned more robust estimates (*i.e.* with a higher snr = μ/σ). This

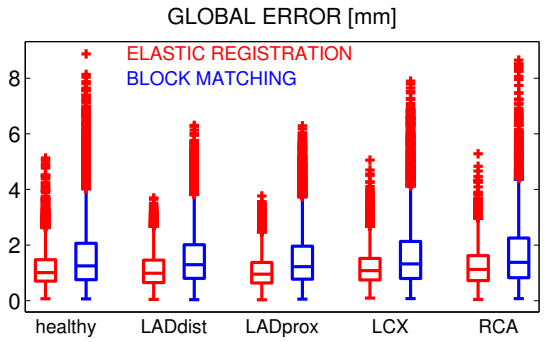

Fig. 2. Global tracking errors for elastic registration (in red) and block matching (in blue) on the five considered sequences. Markers in each box correspond to 25-th, 50-th and 75-th percentile values. Values outside the range +/-3σ are classified as outliers (red pluses).

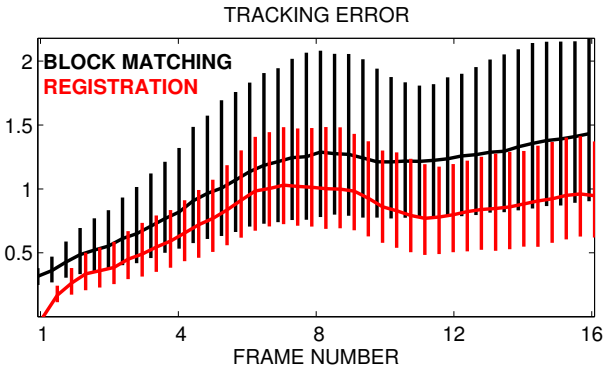

Fig. 3. Tracking error over time. Bold time curves report median errors. Vertical segment denote 25-th and 75-th percentile values.

is clearly due to the intrinsic spatial regularization of the estimated displacement fields. As a consequence, smoother error maps were obtained with elastic registration, cf. Fig. 4.

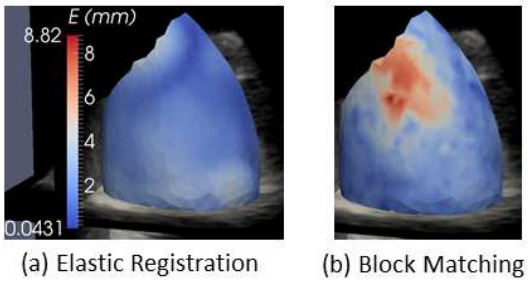

Fig. 4. Error maps for elastic registration (a) and block matching (b) at end-systole of the healthy sequence. Error values are displayed on the ground-truth geometry.

B. Strain accuracy

Correlation plots and Bland-Altman plots of the computed ES circumferential strain are reported in Fig. 5. All sequences were considered at once, *i.e.* 85 sample points (17 segments times 5 sequences) were included in the analysis for each algorithm. The values found for all the strain components are summarized in Table I.

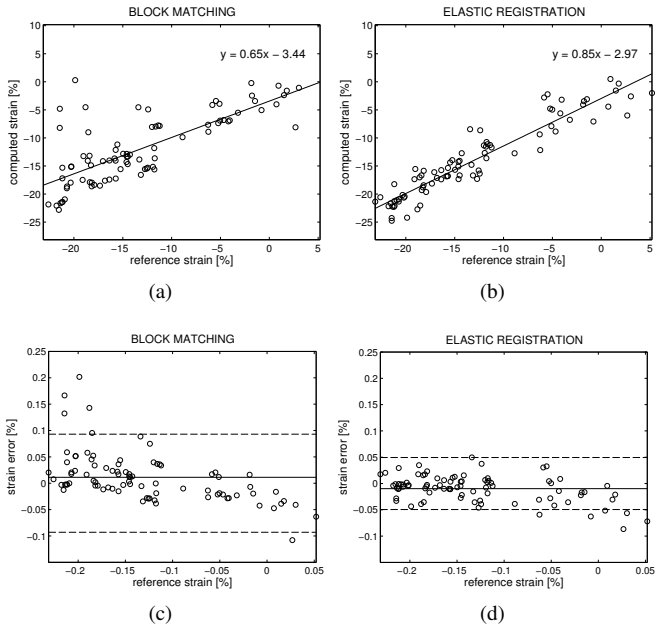

Fig. 5. Correlation (a,b) and Bland-Altman analysis (c,d) for circumferential ES strain estimated with the two techniques considered. The correlation plot also reports the expression of the line fitted in the least-squares sense.

For all the strain components elastic registration returned higher correlation coefficients, lower bias and smaller limits of agreement as compared to block matching. Nevertheless, observed differences were not always statistically significant (cf. Table I). This is likely due to the limited number of samples included in this initial study. For both algorithms, the most reliable strain component was the circumferential one, while significant biases and low correlation values were obtained for the radial component. In agreement with previous studies, this confirms that obtaining reliable estimates of radial displacements is still an open issue.

As a measure of the sensitivity of the two techniques to the presence of akinetic regions, we evaluated how effectively computed strain values could cluster healthy and diseased segments. The results are summarized in Fig. 6. We used the Mahalanobis $M = (\mu_1 - \mu_2)/(\sigma_1 + \sigma_2)$ to evaluate the distance between the two clusters. For all strain components elastic registration produced the best inter-cluster separation (cf. Table II). Nonetheless, both methods performed poorly when R-strain was considered. In line with previous studies, this result confirms that accurate evaluation of radial displacements with ultrasound is still an open issue.

TABLE II. MAHALANOBIS DISTANCE BETWEEN CLUSTERS CORRESPONDING TO HEALTHY AND DISEASED SEGMENTS.

	Reference	BM	Registration
C-strain	1.64	1.09	1.29
R-strain	1.54	0.46	0.74
L-strain	1.12	0.69	0.87

IV. Discussion and Conclusion

The paper presented an initial comparison between elastic registration and block matching techniques for cardiac deformation and strain estimation with 3D ultrasound making use of a novel evaluation pipeline recently proposed by the

TABLE I. CORRELATION COEFFICIENT, BLAND-ALTMAN BIAS μ AND BLAND-ALTMAN LIMITS OF AGREEMENT σ IN THE ESTIMATION OF ES STRAIN. THE p-VALUE BETWEEN BRACKETS REPORTS THE STATISTICAL SIGNIFICANCE OF THE REPORTED VALUE. THE SYMBOL † DENOTES STATISTICAL DIFFERENCE ($p < 0.05$) BETWEEN THE TWO ALGORITHMS.

	R-strain			C-strain			L-strain		
	ρ (p-value)	μ (p-value)	σ	ρ (p-value)	μ (p-value)	σ	ρ (p-value)	μ (p-value)	σ
ELASTIC REGISTRATION	0.74 (<0.001)	-2.55 (0.01)†	17.58	0.94 (<0.001)†	0.98 (<0.001)†	4.94	0.71 (<0.001)	-0.28 (0.25)†	4.44
BLOCK-MATCHING	0.56 (<0.001)	13.12 (<0.001)†	21.67	0.77 (<0.001)†	-1.12 (0.03)†	9.30	0.61 (<0.001)	-0.95 (0.002)†	5.29

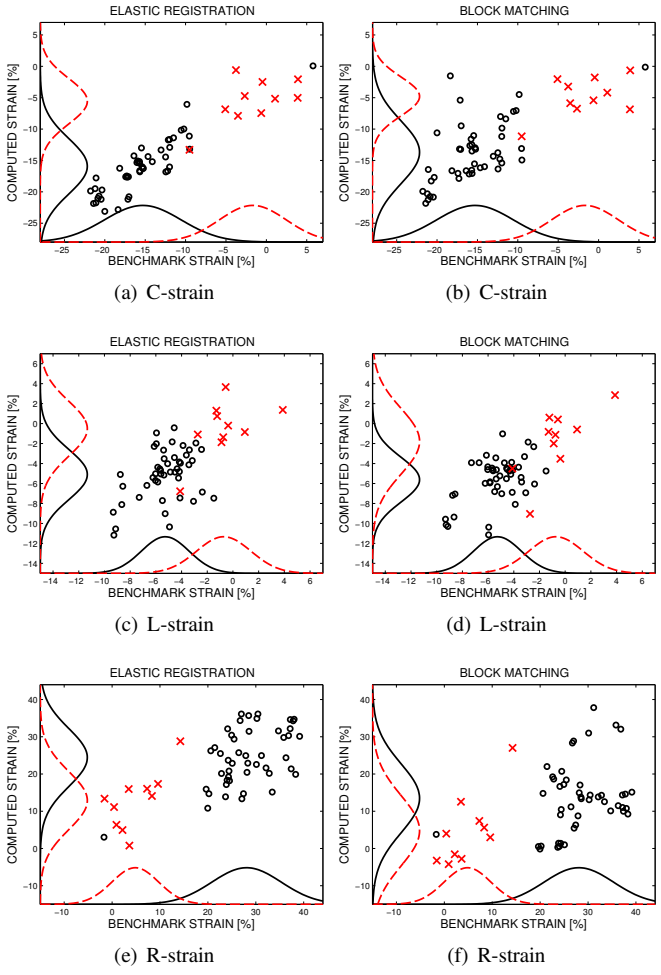

(a) C-strain (b) C-strain

(c) L-strain (d) L-strain

(e) R-strain (f) R-strain

Fig. 6. In the x-axis the reference strain for healthy (in black) and ischemic (in red) segments. In the y-axis the values returned by the estimator. The two best-fit Gaussian curves are reported as an indicator of the separation between the two groups.

authors. The main limitation of this study was that an in-house implementation of block matching was employed where i) no spatial nor temporal smoothing were included, ii) computational efficiency was highly sub-optimal ($\approx$ 6h per sequence). Hereto, in the future it would be of interest to involve commercially available implementations of speckle tracking in the comparison. Moreover, given the reduced size of the dataset, obtained differences were not always statistically significant. A more extensive evaluation is therefore needed, including a wider range of motion patterns and image qualities.

Despite these limitations, this study brings further evidence that elastic registration might represent a valuable alternative to speckle tracking for a reliable estimation of cardiac dynamics and that this novel technique is hence ready for more extensive clinical trials. Future studies include employing the proposed benchmarking pipeline to contrast a wider range of state-of-the art motion estimation solutions.

ACKNOWLEDGMENT

The work of Martino Alessandrini was funded by the Research Foundation Flanders (FWO).

REFERENCES

[1] B. Heyde, R. Jasaityte, D. Barbosa, V. Robesyn, S. Bouchez, P. Wouters, F. Maes, P. Claus, and J. D'hooge, "Elastic image registration versus speckle tracking for 2-d myocardial motion estimation: A direct comparison in vivo," *IEEE TMI*, vol. 32, no. 2, pp. 449–459, 2013.

[2] B. Heyde, D. Barbosa, P. Claus, F. Maes, and J. Dhooge, "Influence of the grid topology of free-form deformation models on the performance of 3d strain estimation in echocardiography," in *proc. of FIMH*, 2013, vol. 7945, pp. 308–315.

[3] R. Jasaityte, B. Heyde, V. Ferferieva, B. Amundsen, D. Barbosa, D. Loeckx, G. Kiss, F. Orderud, P. Claus, H. Torp, and J. Dhooge, "Comparison of a new methodology for the assessment of 3d myocardial strain from volumetric ultrasound with 2d speckle tracking," *The International Journal of Cardiovascular Imaging*, vol. 28, no. 5, pp. 1049–1060, 2012.

[4] M. De Craene, M. Alessandrini, P. Allain, S. Marchesseau, I. Waechter-Stehle, J. Weese, E. Saloux, H. G. Morales, R. Cuingnet, H. Delingette, M. Sermesant, O. Bernard, and J. D'hooge, "Ultra-realistic synthetic echocardiographic sequences for quality assurance of strain estimation algorithms," in *proc. of ISBI 2014*, 2014, pp. 73–76.

[5] S. Marchesseau, H. Delingette, M. Sermesant, M. Sorine, K. Rhode, S. Duckett, C. Rinaldi, R. Razavi, and N. Ayache, "Preliminary specificity study of the Bestel-Clement-Sorine electromechanical model of the heart using parameter calibration from medical images," *J Mech Behav Biomed Mater.*, vol. 20, pp. 259–271, 2013.

[6] H. Gao, H. F. Choi, P. Claus, S. Boonen, S. Jaecques, G. Van Lenthe, G. Van der Perre, W. Lauriks, and J. D'hooge, "A fast convolution-based methodology to simulate 2-d/3-d cardiac ultrasound images," *IEEE TUFFC*, vol. 56, no. 2, pp. 404–409, 2009.

[7] M. D. Cerqueira, N. J. Weissman, V. Dilsizian, A. K. Jacobs, S. Kaul, W. K. Laskey, D. J. Pennell, J. A. Rumberger, T. Ryan, and M. S. Verani, "Standardized myocardial segmentation and nomenclature for tomographic imaging of the heart: A statement for healthcare professionals from the cardiac imaging committee of the council on clinical cardiology of the american heart association," *Circulation*, vol. 105, no. 4, pp. 539–542, 2002.

[8] M. De Craene, S. Marchesseau, B. Heyde, H. Gao, M. Alessandrini, O. Bernard, G. Piella, A. Porras, L. Tautz, A. Hennemuth, A. Prakosa, H. Liebgott, O. Somphone, P. Allain, S. Makram Ebeid, H. Delingette, M. Sermesant, J. D'hooge, and E. Saloux, "3d strain assessment in ultrasound (straus): A synthetic comparison of five tracking methodologies," *IEEE TMI*, vol. 32, no. 9, pp. 1632–1646, 2013.